J Eng Math
DOI 10.1007/s10665-013-9668-z

Unwinding of a cholesteric liquid crystal and bidirectional surface anchoring

G. McKay

Received: 23 January 2013 / Accepted: 16 August 2013

Abstract We examine the influence of bidirectional anchoring on the unwinding of a planar cholesteric liquid crystal induced by the application of a magnetic field. We consider a liquid crystal layer confined between two plates with the helical axis perpendicular to the substrates. We fix the director twist on one boundary and allow for bidirectional anchoring on the other by introducing a high-order surface potential. By minimizing the total free energy for the system, we investigate the untwisting of the cholesteric helix as the liquid crystal attempts to align with the magnetic field. The transitions between metastable states occur as a series of pitchjumps as the helix expels quarter- or half-turn twists, depending on the relative sizes of the strength of the surface potential and the bidirectional anchoring. We show that secondary easy axis directions can play a significant role in the unwinding of the cholesteric in its transition towards a nematic, especially when the surface anchoring strength is large.

Keywords Cholesteric liquid crystal · Helix unwinding · Weak anchoring

1 Introduction

A cholesteric (or chiral nematic) is a type of liquid crystal whose chiral nature causes the constituent molecules to align at a slight angle to one another. This leads to a periodic configuration in which the preferred direction of the long molecular axis (or director) twists continuously in space perpendicular to a helical axis. The length over which the director rotates by 2π radians is known as its pitch and can vary from 200 nm upwards [1, p. 5]. In the absence of any external influences such as an applied field, the cholesteric possesses a natural or equilibrium pitch that depends on the temperature of the liquid crystal. However, due to diamagnetic or dielectric anisotropy, the period of the helical structure can be changed by the application of a magnetic or electric field. De Gennes [2] and Kedney and Stewart [3] predict theoretically how the helix can be completely unwound in an infinite sample of cholesteric liquid crystal, resulting in a cholesteric to homeotropic (planar) nematic phase transition. The same field-induced transition is also observed experimentally by Meyer [4]. Subsequent studies examine the dependence of the observed helical pitch on the field strength and critical fields for complete unwinding [5–8] and allow experimentalists to measure physical quantities, for example, the twist elastic constant of the cholesteric.

G. McKay (✉)
Department of Mathematics and Statistics, University of Strathclyde, Glasgow G1 1XH, UK
e-mail: g.mckay@strath.ac.uk

Published online: 01 October 2013

When considering an infinite sample of cholesteric (i.e. a relatively thick sample in which the bulk is unaffected by any boundary surfaces), the pitch changes continuously, increasing smoothly with the applied field until it becomes infinite and the helix is completely unwound. However, when the liquid crystal has a finite thickness, confined between two substrates with some degree of anchoring on the surfaces, changes in pitch may occur in discrete jumps. These pitchjumps can arise due to changes in the natural pitch with temperature [9–11] and are often associated with thermal hysteresis [12–14]. An applied field can also lead to stepwise changes in pitch and helix unwinding in confined samples [15–18]. Kedney and Stewart [19] present a theoretical analysis of the unwinding of a cholesteric with strong anchoring on the substrates, i.e. the angle of director twist is fixed on the boundaries. As we will discuss in Sect. 3, different metastable states can coexist for a given field strength. The discrete pitchjumps coincide with a change in the nature of the twist profile that provides the global energy minimizer. More recently, Scarfone et al. [20] generalize the problem of [19] to consider an in-plane magnetic field tilted at some angle with respect to fixed parallel twist directions on the substrates. The analysis of Lelidis et al. [21] allows for an incomplete number of half twists in the liquid crystal layer by imposing strong homogeneous anchoring with non-parallel director twists on the two confining plates.

More realistic boundary conditions for liquid crystals allow for the director angle on a boundary to vary because of the competition between the bulk alignment and a preferred surface direction (or easy axis direction). The director is thought to be weakly anchored at the substrate, with a degree of flexibility controlled by a finite anchoring strength combined with a surface energy. Easy axis directions can be imposed on solid substrates via a variety of methods, for example, surface rubbing and oblique evaporation of a SiO thin film on the surface. As the anchoring strength increases, we revert to strong boundary conditions with the direction fixed in the easy axis direction on the substrate, also known as infinite anchoring. Belyakov and co-workers [22–27] present theoretical analyses of the untwisting of a cholesteric due to the action of a field or temperature with weak anchoring on the bounding plates, whereas the stability of the helical structures when there is asymmetry due to different anchoring strengths on the two surfaces is considered by Kiselev and Sluckin [28].

Most of the studies examining discrete jumps in pitch in cholesteric liquid crystal cells bounded by two parallel substrates employ an anchoring potential of the form

$$w_{\mathrm{s}}(\overline{\phi}) = \frac{1}{2}\tau_0 \sin^2 \overline{\phi} \tag{1}$$

on one or both plates, where τ_0 is the anchoring strength and $\overline{\phi}$ is the director azimuthal twist angle at the surface. This is the twist equivalent of the quadratic surface energy density first proposed by Rapini and Papoular [29] and adopted widely in models for liquid crystals [30, p. 49]. The form (1) represents a substrate that is rubbed to provide easy axes for the director at $\overline{\phi} = k\pi$ radians, where k is an integer. The quadratic expansion also ensures that the inversion symmetry of cholesterics is preserved. It is also possible, however, to obtain bidirectional surface ordering in liquid crystal devices with two easy directions on a substrate. This can be achieved via a variety of treatments at the upper surface plate, for example, patterned surfaces [31–33], SiO evaporation [34] and non-parallel aligning films [35]. Mathematically, bistable surface anchoring can be modelled by introducing a higher-order surface potential into (1). The theoretical studies of Sergan and Durand [34], Barberi et al. [35] and Yoneya et al. [36] incorporate a quartic expansion in $\sin\overline{\phi}$,

$$w_{\mathrm{s}}(\overline{\phi}) = \frac{1}{2}\tau_0(\sin^2 \overline{\phi} + \zeta \sin^4 \overline{\phi}). \tag{2}$$

The dimensionless bidirectional coefficient ζ depends on the nature of the interaction between the liquid crystal and the surface, with $\zeta = 0$ corresponding to the quadratic Rapini–Papoular anchoring (1). The higher-order potential (2) still preserves the inversion symmetry of the cholesteric but also provides secondary easy directions corresponding to odd multiples of $\pi/2$ radians when $\zeta < -1/2$. In particular, $\zeta = -1$ provides surface potential minima of equal strength at all integer multiples of $\pi/2$ radians. The quartic form (2) was generalized by Pieranski and Jérôme [37] in a study of discontinuous first-order anchoring transitions by introducing a phase angle in the fourth-order term. McKay [14] employed (2) in a study of the thermal hysteresis of pitchjumps in a planar cholesteric and discusses how the higher-order term can still alter the pitchjump process even when $\zeta > -1/2$. Apart from an

initial discussion about the Rapini–Papoular case $\zeta = 0$, here we concentrate on perpendicular easy directions and $\zeta \approx -1$.

The aim of this paper is to examine the influence of a bidirectional anchoring potential on the unwinding of a cholesteric liquid crystal subject to the application of a magnetic field. We adopt the quartic surface energy (2) on the upper boundary confining a layer of cholesteric while maintaining a strong anchoring condition on the lower surface. In Sect. 2 we introduce the model for the liquid crystal layer, including the elastic energy density and total energy per unit area. We then derive the differential equations from which we obtain the director twist across the layer. Section 3 examines the unwinding of the cholesteric through a series of pitchjumps at critical values of the field strength. These can be quarter- or half-turn changes in the twist angle depending on the choice of bidirectional anchoring parameter ζ and the anchoring strength. We show that the influence of the bidirectional anchoring increases as the anchoring strength increases, although it may still be possible for the unwinding to bypass intermediate easy axis directions when the magnitude of the field is relatively large and the cholesteric is almost completely unwound.

2 Model

We consider a cholesteric liquid crystal of thickness d between two boundary plates at $z = 0$ and $z = d$. Assuming that the nematic director lies in the xy-plane and the helical axis is in the z-direction, the director can be described via

$$\mathbf{n} = \big(\cos\phi(z),\ \sin\phi(z),\ 0\big), \tag{3}$$

where $\phi(z)$ is the director twist angle measured with respect to the x-axis, as shown in Fig. 1. The liquid crystal is subject to an in-plane magnetic field $\mathbf{H} = H(1,\ 0,\ 0)$ of magnitude $H(\geq 0)$.

Combining the magnetic and elastic energy densities, we can express the overall bulk energy density for the cholesteric [38, Chap. 6] as

$$w_{\mathrm{b}} = \frac{1}{2}K_2\Big(\mathbf{n}\cdot\nabla\times\mathbf{n} - \frac{2\pi}{p}\Big)^2 - \frac{1}{2}\chi_a(\mathbf{n}\cdot\mathbf{H})^2 = \frac{1}{2}K_2\Big(\frac{\mathrm{d}\phi}{\mathrm{d}z} - q\Big)^2 - \frac{1}{2}\chi_a H^2\cos^2\phi, \tag{4}$$

where K_2 is the elastic constant associated with twist of the cholesteric and χ_a is the magnetic anisotropy, here assumed to be positive so that the liquid crystal director prefers to align with the field. The wavenumber $q = 2\pi/p$ is also assumed to be positive so that the cholesteric exhibits a right-handed helix. The natural, or equilibrium, pitch p is the distance along the helical axis over which the director twists 2π radians in the absence of the applied field or surface anchoring. On the lower plate at $z = 0$ we assume that the director is fixed such that $\phi(0) = 0$. At the upper surface we introduce the bidirectional surface energy (2), where $\overline{\phi}$ represents the twist on the substrate.

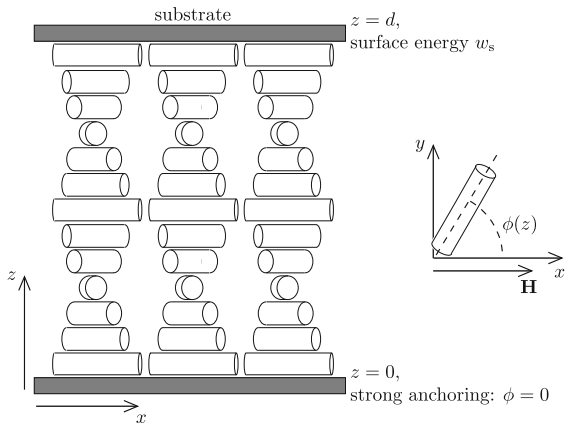

Fig. 1 Cholesteric liquid crystal confined between two plates at $z = 0$ and $z = d$ with its helical axis in z-direction. The director twist with respect to the x-axis direction is $\phi(z)$, while $\mathbf{H}$ is the in-plane magnetic field

Combining the bulk and surface energies, we can now construct the total energy of our system per unit area:

$$W = \int_0^d w_\mathrm{b}\,\mathrm{d}z + w_\mathrm{s}, \tag{5}$$

where w_s is the quartic surface potential (2). Equilibrium profiles for the director twist can be found by minimizing the total energy W with respect to the angle ϕ. Before doing this, we first non-dimensionalize (5) by rescaling $z \to z/d$ and introducing a modified total energy

$$\widehat{W} = \frac{2d}{K_2} W = \int_0^1 \left(\frac{\mathrm{d}\phi}{\mathrm{d}z} - \pi\hat{q}\right)^2 - \lambda^2 \cos^2\phi\,\mathrm{d}z + \frac{2\pi}{\rho}\hat{w}_\mathrm{s} \equiv \int_0^1 \hat{w}_\mathrm{b}\,\mathrm{d}z + \frac{2\pi}{\rho}\hat{w}_\mathrm{s}, \tag{6}$$

where the dimensionless surface energy $\hat{w}_\mathrm{s} = \left(\sin^2\overline{\phi} + \zeta\sin^4\overline{\phi}\right)/2$ and $\overline{\phi}$ still represents the director twist on the upper surface. We have also introduced non-dimensional parameters

$$\rho = \frac{\pi K_2}{d\tau_0}, \quad \hat{q} = \frac{qd}{\pi}, \quad \lambda^2 = \frac{d^2\chi_a H^2}{K_2}.$$

Non-negative ρ is a rescaled reciprocal of the anchoring strength, with $\rho = 0$ corresponding to infinite anchoring. The parameter $\hat{q}$ represents the number of half (or π)-twists in a sample of depth d if the director was allowed to rotate freely on the upper plate (zero anchoring) and the magnetic field is switched off. The helix will attempt to unwind as the magnetic field strength increases, so the actual number of half-twists exhibited by the cholesteric may differ from $\hat{q}$. In order to focus on the competition between the field strength and surface anchoring, we have fixed $\hat{q} = 10$ in Figs. 2–8. Finally, λ is a measure of the magnitude of the magnetic field relative to the twist elastic constant.

We calculate the equilibrium twist profiles for the cholesteric by minimizing the energy $\widehat{W}$. The Euler–Lagrange equation derived from (6) is

$$\frac{\mathrm{d}^2\phi}{\mathrm{d}z^2} - \lambda^2\cos\phi\sin\phi = 0, \quad z \in (0,\,1). \tag{7}$$

The boundary condition for the twist at the upper plate can also be obtained from calculus of variations [39, Chap. 4],

$$\frac{\partial\hat{w}_\mathrm{b}}{\partial\phi'} + \frac{\mathrm{d}\hat{w}_\mathrm{s}}{\mathrm{d}\overline{\phi}} = 0 \quad \text{on } z = 1, \tag{8}$$

where $\phi' = \mathrm{d}\phi/\mathrm{d}z$. Substituting $\hat{w}_\mathrm{b}$ and $\hat{w}_\mathrm{s}$ defined in (6) into (8), we can write the boundary condition for ϕ incorporating weak anchoring as

$$\frac{\mathrm{d}\phi}{\mathrm{d}z} - \pi\hat{q} + \frac{\pi}{\rho}\sin\overline{\phi}\cos\overline{\phi}(1 + 2\zeta\sin^2\overline{\phi}) = 0 \quad \text{on } z = 1. \tag{9}$$

Equilibrium twist profiles are now solutions of (7) and (9), in conjunction with the condition that the angle vanishes at $z = 0$.

Following a procedure similar to that adopted in Kedney and Stewart [3] and Scarfone et al. [20], we can obtain an implicit form for $\phi(z)$ from (7),

$$\mathcal{F}(\phi,\,k) - \lambda z = 0, \tag{10}$$

where $k(>0)$ is a constant of integration to be determined,

$$\mathcal{F}(\phi,\,k) = \int_0^\phi \frac{\mathrm{d}\psi}{\sqrt{k + \sin^2\psi}} = \frac{1}{\sqrt{k}} F\left(\phi \mid -k^{-1}\right) \tag{11}$$

and $F(\phi\,|\,m)$ is the incomplete elliptic integral of the first kind. The limiting value of $z = 1$ in (10) provides an implicit form relating k and $\overline{\phi} = \phi(1)$, the twist on the upper plate,

$$\mathcal{F}(\overline{\phi},\,k) - \lambda = 0. \tag{12}$$

However, if we replace the derivative at $z = 1$ in (9) by the term derived from (10), we can obtain another expression for the constant k in terms of $\overline{\phi}$, namely

$$k = \frac{1}{\lambda^2}\left(\pi\hat{q} - \frac{\pi}{\rho}\frac{\mathrm{d}\hat{w}_\mathrm{s}}{\mathrm{d}\overline{\phi}}\right)^2 - \sin^2\overline{\phi}. \tag{13}$$

Together, (12) and (13) provide the constant k and the angle $\overline{\phi}$ corresponding to the chosen non-dimensional parameters ρ, $\hat{q}$ and λ. These lead, in turn, to an implicit form for $\phi(z)$ from (10).

3 Discussion

In Fig. 2a we plot the constant k obtained from both the implicit form (12) and condition (13) for the simple Rapini–Papoular energy (1) as $\overline{\phi}$ varies. Note that the graph derived from (13) is restricted to the values of $\overline{\phi}$ that provide $k > 0$. Figure 2b represents the non-dimensional energy $\widehat{W}$ introduced in (6) for the same range of $\overline{\phi}$, with the values of k calculated using (12). The intersections of the curves in Fig. 2a correspond to energy extrema in Fig. 2b. The magnetic field contribution to the total energy is minimized when the director is aligned in directions which are integer multiples of π radians. Therefore, as the magnetic field strength increases and dominates the elastic or weak anchoring effects, the cholesteric undergoes a series of transitions as its helix unwinds in an attempt to align with the magnetic field. Since multiple metastable states can coexist for a given λ, the pitchjumps coincide with discrete changes in the overall twist of the energy global minimizer. The value of λ chosen in Fig. 2 coincides with a pitchjump as the helix expels approximately a half (or π)-twist and aligns with the field in more of the cell. Figure 3 plots the equilibrium twist profiles $\phi(z)$ obtained from (10)–(13) for a sequence of critical values of the parameter λ. In the analysis that follows we refer to *quarter-* and *half-turn* changes in the overall twist across the entire cell, i.e. variations in the director angle at the upper plate. In reality, these jumps will not be exact integer multiples of $\pi/2$ or π radians, respectively, because of the weak anchoring. We can categorize each profile in Figs. 2 and 3 by n, the number of half-twists it possesses, or simply $\overline{\phi}/\pi$, rounded to the nearest integer multiple of 0.5. For

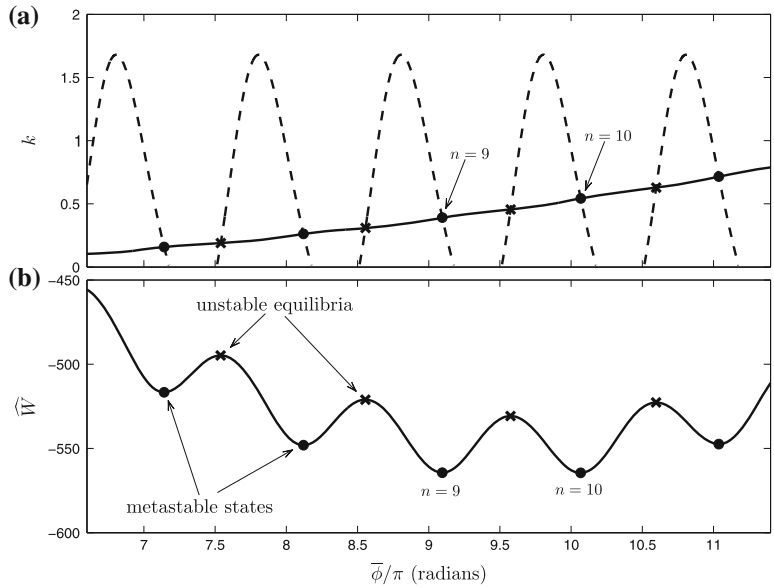

Fig. 2 **a** Constant of integration k derived from implicit Eq. (12) (*solid line*) and boundary condition (13) (*dashed line*) as angle $\overline{\phi}$ varies, with $\lambda = 32.58$, $\rho = 0.1$, $\zeta = 0$ and $\hat{q} = 10$. **b** Energy $\widehat{W}$, where k is calculated using the implicit form (12). Intersections of k-curves coincide with energy extrema and allow us to calculate the energy profile $\phi(z)$ via (10)

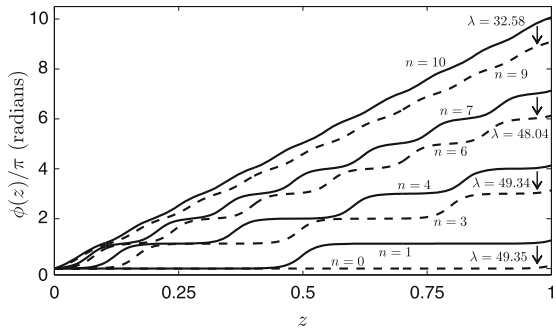

Fig. 3 Unwinding of director twist $\phi(z)$ at specific values of parameter λ with $\rho = 0.1$, $\zeta = 0$ and $\hat{q} = 10$. In each case, the chosen λ corresponds to a critical value where the helix expels a half-twist as the cholesteric unwinds. For each profile, n represents the number of half-twists rounded to the nearest integer multiple of 0.5

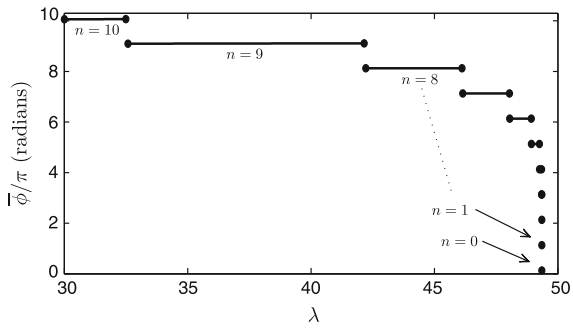

Fig. 4 Azimuthal twist angles at upper plate for variable parameter λ, with $\rho = 0.1$, $\zeta = 0$ and $\hat{q} = 10$. As the field strength increases, the global minimum energy state expels (approximate) half-twists and the cholesteric helix unwinds. The cascade of pitchjumps from $n = 4$ to $n = 0$ takes place over a very short interval when λ is large and the helix is nearly unwound. Note, as seen in Fig. 3, the twist angles at the upper surface are close but not equal to integer multiples of π radians because of the weak anchoring condition

example, the pitchjump at $\lambda = 32.58$ corresponds to a transition from an $n = 10$ to an $n = 9$ state. Figure 4 shows the full cascade of transitions as the field strength increases until the cholesteric is virtually completely unwound, although a small residual twist remains at the upper surface for the $n = 0$ state due to the finite surface energy and elastic effects. As the magnetic field strength is increased even further, this residual surface twist will decrease towards zero.

The quadratic term in the surface energy (2) is minimized when the surface twist aligns at an integer multiple of π radians, in a fashion similar to the director in the bulk of the liquid crystal cell when acted upon by the field. However, if we introduce bidirectional surface anchoring by including the quartic term in (2) for $\zeta < -1/2$, then the new intermediate surface energy minima at odd multiples of $\pi/2$ radians will compete with the magnetic field alignment. Figure 5 shows the intersections of the k-curves and the corresponding energy $\widehat{W}$ in the presence of bidirectional anchoring with $\zeta = -1$. The oscillations in the curve obtained from (13) result in intermediate twist profiles and secondary metastable states corresponding to $n = 10.5,\ 9.5$, etc. This is illustrated further in Fig. 6 for contrasting values of the surface anchoring parameter ρ. For the relatively strong anchoring condition ($\rho = 10^{-4}$), most of the intermediate metastable states act as the global energy minimizer at some stage as λ increases. The step unwinding of the cholesteric occurs in $\pi/2$ pitchjumps until the liquid crystal is almost fully unwound, with only the final intermediate states $n = 3.5$ to $n = 0.5$ skipped when λ is large. Significantly, for the weaker surface anchoring $\rho = 10^{-2}$, a reduced number of the intermediate twists play a role in the cascade of pitchjumps. At higher magnetic fields, the cholesteric bypasses the secondary easy axis directions and unwinds in an extended series of half- instead of quarter-twist pitchjumps at the upper surface.

Figure 7 examines the influence of the anchoring strength in determining whether the director twist will bypass one or more of the intermediate metastable states as the helix unwinds. Critical values of λ are plotted for each pitchjump transition and variable ρ. The branches of Fig. 7 demarcate the regions in $(\lambda,\ \rho)$ space corresponding to the different n-states. For a fixed ρ, we can determine the sequence of unwound twists as λ increases in a manner similar to that in Figs. 4 and 6. We observe from Fig. 7 that the intermediate states at odd multiples of $\pi/2$ radians play a diminishing role as ρ increases. When the anchoring strength is relatively weak, the magnetic and bulk elastic terms dominate the energy of the system, especially for large field strengths. The field prefers to align at integer multiples of π radians and, consequently, the surface energy can no longer constrain the upper surface twist to an angle close to a secondary easy axis direction. As a result, helix unwinding takes place via a series of half-twist pitchjumps focussed on the integer n states. For mid-strength anchoring, quarter-turn pitchjumps may occur initially as the helix unwinds but are bypassed at higher fields, as also shown previously in Fig. 6.

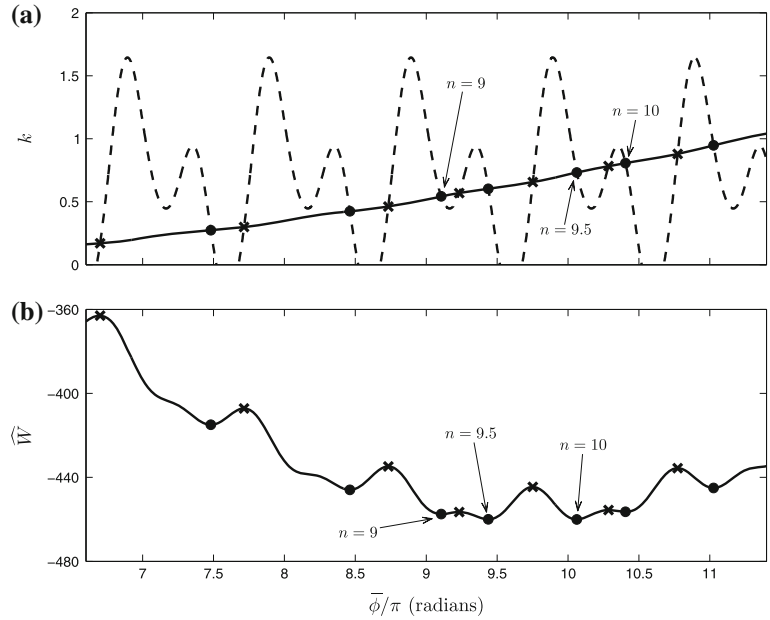

Fig. 5 **a** Constant of integration k derived from implicit Eq. (12) (*solid line*) and boundary condition (13) (*dashed line*) as angle $\overline{\phi}$ varies, with $\lambda = 29.50$, $\rho = 0.1$, $\zeta = -1$ and $\hat{q} = 10$. **b** Energy $\widehat{W}$, where k is calculated using implicit form (12). Oscillations in k-curve obtained from (13) result in secondary metastable states

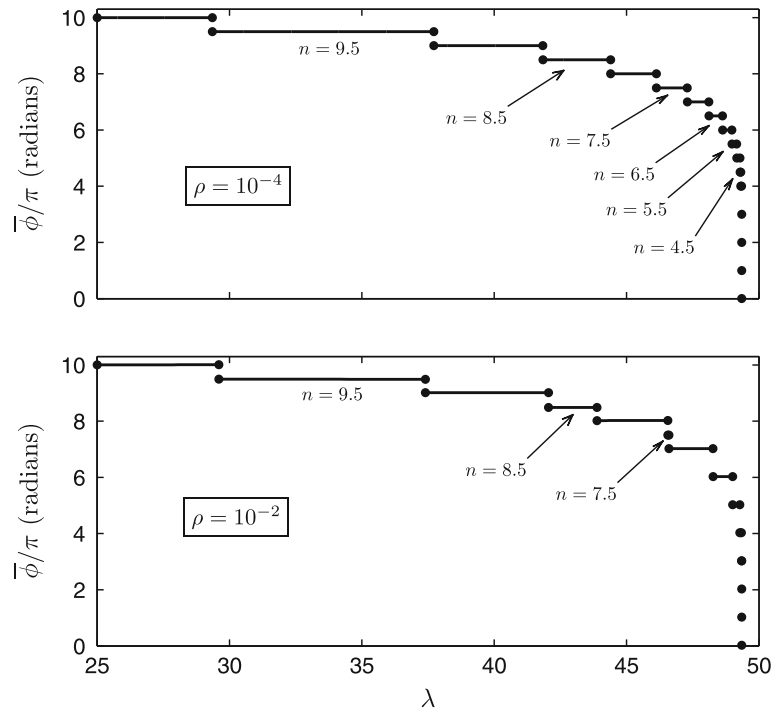

Fig. 6 Azimuthal twist angles at upper plate for $\zeta = -1$, $\hat{q} = 10$ and variable λ. The surface twist now displays values close to the secondary easy directions at odd multiples of $\pi/2$ radians as the helix untwists. When $\rho = 10^{-4}$, the secondary pitchjumps persist until the final transitions when λ is large. For $\rho = 10^{-2}$, which corresponds to weaker anchoring, only the higher-twist intermediate states are observed as the helix unwinds

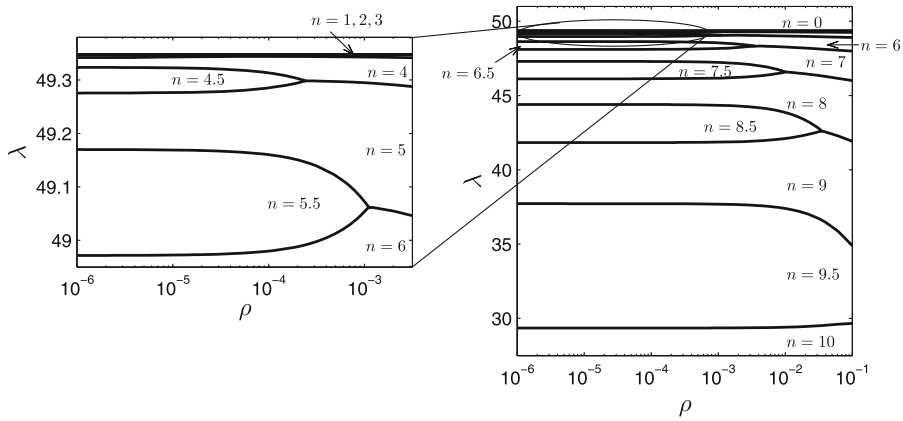

Fig. 7 Regions in $(\lambda,\ \rho)$ space where different n-states act as global energy minimum for $\zeta = -1$, $\hat{q} = 10$. The states $n = 1,\ 2$ and 3 occur in the small region before the helix unwinds but cannot be distinguished in the figure

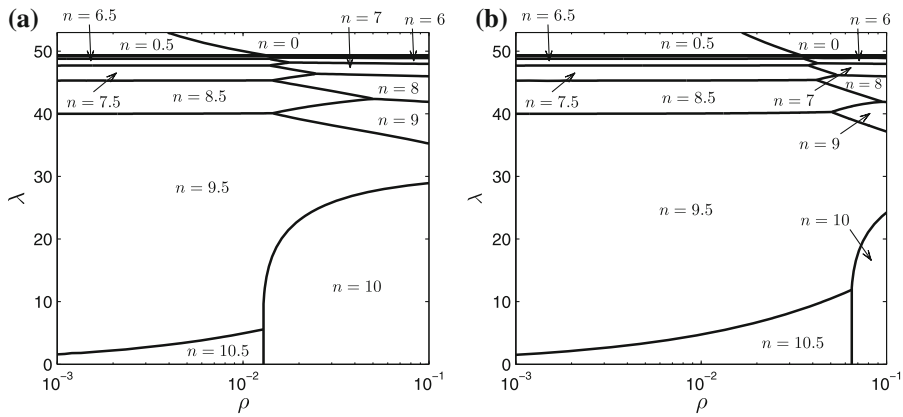

Fig. 8 Regions in $(\lambda,\ \rho)$ space where different n-states are global energy minimum for $\hat{q} = 10$: **a** $\zeta = -1.01$; **b** $\zeta = -1.1$. As ζ decreases, the secondary states dominate the cholesteric transition to a planar nematic

The surface energy term in (6) is very sensitive to the choice of ζ, as can be seen by re-expressing $\hat{w}_s$ in the form

$$\hat{w}_s = \frac{1}{8}\sin 2\overline{\phi} + \frac{1}{2}(\zeta + 1)\sin^4\overline{\phi}. \tag{14}$$

The first term in (14) vanishes for *all* easy directions $\overline{\phi} = k\pi/2$ ($k \in \mathbb{Z}$). However, when combined with the $2\pi/\rho$ coefficient in (6), the second term can be significantly large in magnitude for $\overline{\phi}$ close to the secondary easy axes (odd integer k). Generally, if ζ is slightly greater than -1, then the surface energy contribution to (6) is positive for all secondary states and large enough to ensure that these secondary states never act as global energy minima, i.e. the $n = 9.5,\ 8.5\ \ldots$ regions in Fig. 7 shrink very rapidly as ζ increases from -1. Conversely, the secondary states encroach further into $(\lambda,\ \rho)$ space, even if ζ is decreased by only a relatively small amount. In Fig. 8 we consider the effect of a small decrease in the bidirectional coefficient from $\zeta = -1$, biasing the surface energy towards the secondary directions at odd multiples of $\pi/2$ radians on the boundary. Unlike the situation for $\zeta \geq -1$, this bias can lead to equilibrium states with $n = 10.5$ when the magnetic field is relatively weak and $n = 0.5$ when λ is large and the cholesteric is almost fully unwound. More significantly, it is the secondary states which now play the dominant role and across a much wider range of ρ than when $\zeta = -1$. Integer n states that characterize the influence of the magnetic field are excluded from the unwinding process until ρ and λ are relatively large. Figures 7 and 8 both illustrate that the secondary easy axis directions are prevalent when the anchoring strength is relatively large. More

significantly, the figures also show how even very small changes in the nature of the surface potential, with a shift in bias from primary to secondary easy axis directions, can affect the manner in which the helix unwinds.

4 Conclusion

We have examined the unwinding of a planar cholesteric liquid crystal subject to bidirectional anchoring on its upper plate. By determining the states which minimize the total free energy described in terms of the director twist angle, we have modelled the unwinding of the cholesteric helix via a series of near quarter- or half-turn pitchjumps depending on the choice of bidirectional coefficient. In the transition to the nematic state, a competition exists between the twist angles favoured by the magnetic field and the easy axis directions imposed by the surface potential. Secondary easy axes can influence the unwinding when the surface anchoring strength is relatively strong and when the potential is biased towards secondary twisted states via the coefficient ζ. Although not considered here, the behaviour of a cholesteric as it transitions to the nematic state could also be altered by a surface treatment which leads to non-perpendicular easy directions. Another method of controlling the nature of the helix as it unwinds could be the application of an in-plane magnetic field that is tilted with respect to the easy axes, as considered by Scarfone et al. [20] for Rapini–Papoular anchoring. For example, consider a magnetic field that is tilted at a specific angle and whose strength is increased until the cholesteric helix has unwound. If the tilt angle is then changed by a small amount and the field strength decreased, then the helix rewinding may be characteristically different from the unwinding process because the field is more closely aligned with a different easy direction.

References

1. de Jeu WH (1980) Physical properties of liquid crystalline materials. Gordon and Breach, New York
2. de Gennes PG (1968) Calcul de la distorsion d'une structure cholesterique par un champ magnetique. Solid State Commun 6:163–165
3. Kedney PJ, Stewart IW (1994) On the magnetically induced cholesteric to nematic phase transition. Lett Math Phys 31:261–269
4. Meyer RB (1968) Effects of electric and magnetic fields on the structure of cholesteric liquid crystals. Appl Phys Lett 12:281–282
5. Wysocki J, Adams J, Haas W (1968) Electric-field-induced phase change in cholesteric liquid crystals. Phys Rev Lett 20:1024–1026
6. Meyer RB (1969) Distortion of a cholesteric structure by a magnetic field. Appl Phys Lett 14:208–209
7. Durand G, Leger L, Rondelez F, Veyssie M (1969) Magnetically induced cholesteric to nematic phase transition in liquid crystals. Phys Rev Lett 22:227–228
8. Baessler H, Labes MM (1968) Relationship between electric field strength and helix pitch in induced cholesteric-nematic phase transitions. Phys Rev Lett 21:1791–1793
9. Pinkevich IP, Reshetnyak VY, Reznikov YA, Grechko LG (1992) Influence of light induced molecular conformational transformations and anchoring energy on cholesteric liquid crystal pitch and dielectric properties. Mol Cryst Liq Cryst Sci Technol Sect A 222:269–278
10. Gandhi JV, Mi X-D, Yang D-K (1998) Effect of surface alignment layers on the configurational transitions in cholesteric liquid crystals. Phys Rev E 57:6761–6766
11. Anderson MR, Baughn JW (2004) Hysteresis in liquid crystal thermography. J Heat Transf 126:339–346
12. Palto SP (2002) On mechanisms of the helix pitch variation in a thin cholesteric layer confined between two surfaces. JETP 94:260–269
13. Yoon HG, Roberts NW, Gleeson HF (2006) An experimental investigation of discrete changes in pitch in a thin, planar chiral nematic device. Liq Cryst 33:503–510
14. McKay G (2012) Bistable surface anchoring and hysteresis of pitch jumps in a planar cholesteric liquid crystal. Eur Phys J E 35:74
15. Dreher R (1973) Remarks on the distortion of a cholesteric structure by a magnetic field. Solid State Commun 13:1571–1574
16. van Sprang HA, van de Venne JLM (1985) Influence of the surface interaction on threshold values in the cholesteric-nematic phase transition. J Appl Phys 57:175–179
17. Schlangen LJM, Pashai A, Cornelissen HJ (2000) The field-induced cholesteric-nematic phase transition and its dependence on layer thickness, boundary conditions, and temperature. J Appl Phys 87:3723–3729
18. Smalyukh II, Senyuk BI, Palffy-Muhoray P, Lavrentovich OD, Huang H, Gartland EC, Bodnar VH, Kosa T, Taheri B (2005) Electric-field-induced nematic-cholesteric transition and three-dimensional director structures in homeotropic cells. Phys Rev E 72:061707
19. Kedney PJ, Stewart IW (1994) The untwisting of a bounded sample of cholesteric liquid crystal. Continuum Mech Thermodyn 6:141–148

20. Scarfone AM, Lelidis I, Barbero G (2011) Cholesteric-nematic transition induced by a magnetic field in the strong-anchoring model. Phys Rev E 84:021708
21. Lelidis I, Barbero G, Scarfone AM (2012) Cholesteric pitch-transitions induced by a magnetic field in a sample containing incomplete number of pitches. Cent Eur J Phys 3:587–593
22. Belyakov VA (2002) Untwisting of the helical structure in a plane layer of chiral liquid crystal. JETP Lett 76:88–92
23. Zink H, Belyakov VA (1996) Temperature variations in the director orientation and anchoring energy at the surface of cholesteric layers. JETP Lett 63:43–49
24. Zink H, Belyakov VA (1997) Temperature hysteresis of the change in the cholesteric pitch and surface anchoring in thin planar layers. JETP 85:285–291
25. Zink H, Belyakov VA (1999) Studies of the temperature-pitch variations in planar cholesteric layers and surface anchoring. Mol Cryst Liq Cryst Sci Technol Sect A 329:457–464
26. Belyakov VA, Stewart IW, Osipov MA (2004) Dynamics of jumpwise temperature pitch variations in planar cholesteric layers for a finite strength of surface anchoring. JETP 99:73–82
27. Belyakov VA, Stewart IW, Osipov MA (2005) Surface anchoring and dynamics of jump-wise director reorientations in planar cholesteric layers. Phys Rev E 71:051708
28. Kiselev AD, Sluckin TJ (2005) Twist of cholesteric liquid crystal cells: stability of helical structures and anchoring energy effects. Phys Rev E 71:031704
29. Rapini A, Papoular M (1972) Distortion d'une lamelle nematique sous champ magnetique conditions d'ancrage aux parois. J de Physique Colloq 30(C4):54–56
30. Stewart IW (2004) The static and dynamic continuum theory of liquid crystals. Taylor and Francis, London
31. Kim J-H, Yoneya M, Yamamoto J, Yokoyama H (2001) Surface alignment bistability of nematic liquid crystals by orientationally frustrated surface patterns. Appl Phys Lett 78:3055–3057
32. Fukuda J, Yoneya M, Yokoyama H (2007) Surface-groove-induced azimuthal anchoring of a nematic liquid crystal: Berreman's model re-examined. Phys Rev Lett 98:187803
33. Gwag JS, Fukuda J, Yoneya M, Yokoyama H (2007) In-plane bistable nematic liquid crystal devices based on nanoimprinted surface relief. Appl Phys Lett 91:073504
34. Sergan V, Durand G (1995) Anchoring anisotropy of a nematic liquid crystal on a bistable SiO evaporated surface. Liq Cryst 18:171–174
35. Barberi R, Bonvent JJ, Giocondo M, Iovane M (1998) Bistable nematic azimuthal alignment induced by anchoring competition. J Appl Phys 84:1321–1324
36. Yoneya M, Kim JH, Yokoyama H (2002) Simple model for patterned bidirectional anchoring of nematic liquid crystal and its bistability. Appl Phys Lett 80:374–376
37. Pieranski P, Jérôme B (1989) Adsorption-induced anchoring transitions at nematic–liquid–crystal–crystal interfaces. Phys Rev A 40:317–322
38. de Gennes PG, Prost J (1993) The physics of liquid crystals, 2nd edn. Clarendon, Oxford
39. Courant R, Hilbert D (1953) Methods of mathematical physics, vol 1. Interscience, New York